DEPTH PROFILES OF COSMOGENIC 81KR AND LIGHT NOBLE GASES IN THE CHELYABINSK (LL5) METEOROID. K. Nagao[1*], J. Choi[1,2], J. M. Baek[1], J. Park[3,4,5], G. F. Herzog[4], V. Grokhovsky[6], L. E. Nyquist[7], C.-Y. Shih[8], J. I. Lee[1,2], C. Park[1], M. J. Lee[1], [1]Korea Polar Research Institute (KOPRI), 26 Songdomirae-ro, Yeonsu-gu, Incheon 21990, South Korea, [2]University of Science and Technology, 217 Gajeong-ro, Yuseong-gu, Daejeon 34113, South Korea, [3]Kingsborough Community College, Brooklyn, NY 11235, USA, [4]Department of Chemistry & Chemical Biology, Rutgers University, Piscataway, NJ 08854, USA, [5]American Museum of Natural History (AMNH), NY, NY 10024, USA. [6]Institute of Physics and Technology, Ural Federal University, Ekaterinburg, 620002, Russia. [7]R/NASA Johnson Space Center, Houston, TX 77058, USA, [8]16406 Locke Haven, Houston, TX 77059, USA.

Introduction: The Chelyabinsk meteorite fell as a large fireball in Russia on February 15, 2013 and was classified as LL5 chondrite. Numerous small fragments as well as a few much heavier ones (> 100 kg) have been recovered. These fragments derived from different depths in a very large meteoroid, perhaps ~20 m in diameter [see 1]. Many geochemical, mineralogical, and petrological studies have been reported [e.g., 2, 3, 4, 5, 6] and a short cosmic ray exposure (CRE) age of about 1.2 Ma has been determined [e.g., 1, 7, 8, 9]. Because the fragments come from different depths the calculations of CRE age must correct for differences in production rates due to shielding variations under 2π-geometry. In an object with CREage of 1.2 Ma, the ^{81}Kr ($T_{1/2}$ = 0.23 Ma) concentration should reach 97% of their maximum possible (saturation) values and provide one measure of shielding. In [1] cosmogenic ^{81}Kr was determined for one bulk sample, HR-7, and the shielding of this sample was deduced from a consideration of the ^{81}Kr depth profile of a lunar core sample determined by [10]. The production rate of cosmogenic ^{21}Ne and a CRE age were calculated for the sample HR-7 following [10].

We measured all stable noble gas isotopes of He, Ne, Ar, Kr and Xe, and ^{81}Kr for 12 Chelyabinsk fragments, HR-1 to HR-12, which derived from depths ranging from the surface to ≈3m [1, 8], and from light and dark lithologies from the main mass (MM-light and MM-dark) recovered from the Lake Chebarkul [11]. We present depth profiles of ^{81}Kr concentrations along with those of cosmic-ray- produced light noble gases, and discuss the cosmic ray exposure of this large meteoroid.

Experimental method: Bulk samples weighing 275–435 mg were prepared from the above mentioned 14 fragments for noble gas analyses. The samples were installed into a glass sample holder attached to a furnace for noble gas extraction, and then heated to 150°C under ultra-high vacuum for about a day to desorb atmospheric contamination. Each sample was dropped into a Mo-crucible and heated at 1800°C to extract noble gases. The noble gases were purified with two Ti-Zr getters heated at about 750°C and two SAES getters (NP-10), then separated into five fractions mainly composed of He, Ne, Ar, Kr, and Xe. The abundance and isotopic compositions of each fraction were measured with the modified-VG5400 noble gas mass spectrometer at Korea Polar Research Institute (KOPRI) [12]. Mass discrimination effects and sensitivities of the mass spectrometer were determined by measuring known amounts of an atmosphere and a laboratory standard ^{3}He-^{4}He mixture. Blank levels (in cm^{3}STP) were 7.4×10^{-11} (^{4}He), 1.7×10^{-12} (^{20}Ne), 1.3×10^{-9} (^{40}Ar), 1.0×10^{-13} (^{84}Kr), and 1.4×10^{-14} (^{132}Xe). Blank correction was applied for all noble gas isotopes, although the corrections were less than 1%. Signal intensities at ^{79}Br, ^{81}Kr, and ^{84}KrH were similar to 1×10^{-17} cm^{3}STP, and approximately at the detection limit of our mass spectrometer. However, based on the signal intensities at ^{79}Br and ^{84}KrH measured for each sample, ^{81}Kr was corrected for ^{81}Br (^{79}Br = ^{81}Br) and ^{80}KrH (= ^{80}Kr × ^{84}KrH/^{84}Kr). The uncertainty of sensitivities for all noble gas elements was conservatively assumed to be 10%, although the observed variations of sensitivities were smaller.

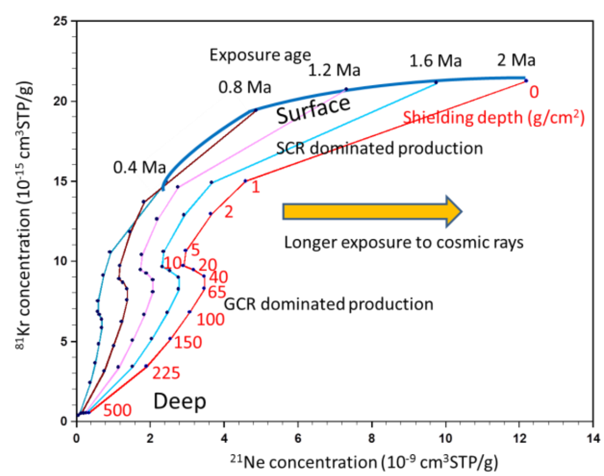

Fig. 1. Model calculations [9] of depth-dependent growth curves of cosmogenic ^{81}Kr and ^{21}Ne; both SCR and GCR are included.

Cosmogenic ^{21}Ne and ^{81}Kr concentrations of $(2.74\pm0.27)\times10^{-9}$ and $(17.3\pm2.7)\times10^{-15}$ cm^3STP/g, respectively, for HR-7 (381.27 mg) measured in this work agree well with $(2.76\pm0.28)\times10^{-9}$ and $(15.8\pm1.9)\times10^{-15}$ cm^3STP/g measured for HR-7 (501.8 mg) in 2013 in Tokyo [8].

Results and discussion:

Depth-dependent growth curve of cosmogenic ^{81}Kr and ^{21}Ne under 2π-irradiation. Fig. 1 shows the expected concentrations of radioactive ^{81}Ke and stable ^{21}Ne as modeled by [9] for different shielding depths and assumed CRE ages. The model includes the effects of both solar cosmic rays (SCR) and galactic cosmic rays (GCR). For target element concentrations, the elemental compositions in [2] were adopted in the calculation. Because of the relatively short exposure age (≈1.2 Ma) of the Chelyabinsk meteoroid, ^{81}Kr concentration in surface layer is slightly below the saturation level of about 2.1×10^{-15} cm^3STP/g. Rapid decrease of both ^{81}Kr and ^{21}Ne in the near-surface layer (<10 cm) is due to rapid decrease of the flux of low energy SCR particles; at larger depths, production by GCR becomes dominant.

^{81}Kr versus ^{21}Ne and ^{38}Ar. Concentrations of ^{81}Kr versus ^{21}Ne are plotted in Fig. 2 with the depth dependent growth curves shown in Fig. 1. Production rates of ^{21}Ne at different shielding depths are expressed as a curve labeled as 1 Ma exposure age. Analogous plots of ^{81}Kr versus ^{38}Ar are shown in Fig. 3. The wide range of concentrations and positive correlations of cosmogenic ^{81}Kr, ^{21}Ne, and ^{38}Ar plotted in Figs. 2 and 3 show that these samples were bombarded by both SCR and GCR in different shielding depths in the preatmospheric body.

Most samples plotted around the shielding depths of several g/cm^2 are plotted on 1 Ma line, consistent with the reported exposure age of ≈1.2 Ma. In contrast to these data, the samples (HR-1 and HR-2) in heavier shielding depths (>100 g/cm^2) tend to plot on the lines for shorter exposure age (<0.8 Ma), and the samples (e.g., HR-3, HR-4, HR-7, HR-9) plot above the line of 0.6 Ma. This might be a result of recent increase of SCR intensity at the uppermost surface layer of preatmospheric body caused by an erosive loss of surface materials. However, because $^{21}Ne/^{22}Ne$ ratios of 0.828–0.910 for these samples are in the range produced by GCR, other mechanism to enhance ^{81}Kr production might have to be considered.

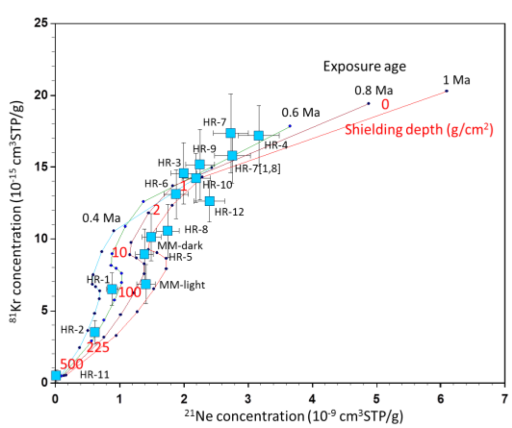

Fig. 2. ^{81}Kr versus ^{21}Ne for HR1–HR12, and MM-light and MM-dark from the Chelyabinmsk LL5

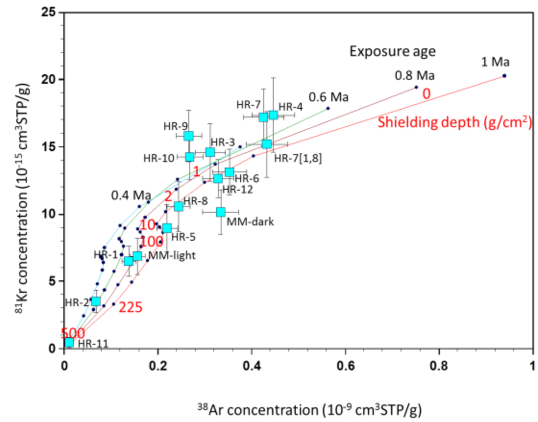

Fig. 3. ^{81}Kr versus ^{38}Ar for HR1–HR12, and MM-light and MM-dark from the Chelyabinmsk LL5 meteorite.

Erosive loss of surface materials of small asteroids with weak gravitational force has been suggested based on short cosmic ray exposure age of the Hayabusa samples returned from the asteroid Itokawa, i.e., <8 Ma [13] and 1.2 Ma [14]. Both Itokawa and Chelyabinsk are LL5 type chondritic bodies, heavily shocked and thus mechanically weak. These results may suggest that surface erosion loss from small meteoroids is common phenomena.

References: : [1] Popova O. P. *et al.* (2013) *Science* **342**, 1069–1073. [2] Galimov E. M. et al. (2013) *ISSN 0016-7029, Geochemistry International* 51, 522-539. [3] Pillinger C. T. et al. (2013) *ISSN 0016-7029, Geochemistry International* 51, 540-548. [4] Righter K. et al. (2013) *76th MetSoc*, Abstract#5235. [5] Yoshida S. et al. (2014) *45th LPSC*, Abstract#2509. [6] Righter K. et al. (2015) *MAPS*, 50, 1790-1819. [7] Nishiizumi K. et al. (2013) *76th MetSoc*, Abstract#5260. [8] Haba M. K. et al. (2014) *45th LPSC*, Abstract#1732. [9] Povinec P. P. *et al.* (2015) *MAPS*, 50, 273-286. [10] Hohenberg et al. (1978), *Proc. Lunar Planet, Sci. Conf. 9th*, 2311–2344. [11] Kocherov A. V. et al. (2014) *45th LPSC*, Abstract #2227. [12] Nagao K. et al. (2017) *48th LPSC*, Abstract#1848. [13] Nagao K. et al. (2011) *Science*, 333, 1128-1131. [14] Meier M. M. M. et al. (2014) *45th LPSC*, Abstract#1247.